

Inhibition of Glyoxalase I: The First Low-Nanomolar Tight-Binding Inhibitors

Swati S. More[†] and Robert Vince*

Center for Drug Design, Academic Health Center, and Department of Medicinal Chemistry, College of Pharmacy, University of Minnesota, 8-123A Weaver Densford Hall, 308 Harvard Street SE, Minneapolis, Minnesota 55455. [†]Current address: Department of Biopharmaceutical Sciences, University of California, San Francisco, San Francisco, CA 94158. Phone: 415-514-4363. E-mail: swati.more@ucsf.edu.

Received April 22, 2009

A series of rational modifications to the structure of known *S*-(*N*-aryl-*N*-hydroxycarbamoyl)glutathione-based glyoxalase I inhibitors culminated in the discovery of the first single-digit nanomolar inhibitor. This study makes available key information about possible means to address the issues of metabolic instability, low potency, and synthetic complexity that have plagued the area of glyoxalase I inhibition. Knowledge garnered from this study has implications in the design of inhibitors with higher conformational definition and lower peptidic character.

Introduction

Glycolysis results in a number of electrophilic carbonyl compounds such as glyoxal, methylglyoxal (MG), and 3-deoxyglucosone, which are capable of forming adducts with proteins, lipids, and nucleic acids. Such adducts, collectively known as advanced glycation end-products (AGEs),¹ are inducers of apoptosis. Several mechanisms exist to protect the cellular components against such “carbonyl stress”, one of them being the glyoxalase system that converts methylglyoxal, the simplest of the α -ketoaldehydes, to *D*-lactate. Depicted in Figure 1, the system is composed of two enzymes; glyoxalase I (Glx-I, EC 4.4.1.5) and glyoxalase II (Glx-II, EC 3.1.2.6). Glx-I mediates the enolization of the hemithioacetal of glutathione with glyoxal to an enediol(ate). This process amounts to a net transfer of a hydride from the methine carbon of the hemiacetal of methylglyoxal and glutathione to the ketone carbonyl, thereby resulting in the formation of *S*-*D*-lactoyl glutathione. Glx-II then hydrolyzes this labile thioester to *D*-lactate, regenerating glutathione.² A feedback mechanism exists between glycolysis and detoxification systems such as the glyoxalase system. The proper function of this feedback mechanism is essential to the prevention of apoptosis.

A hallmark of rapid tumor growth is increased glycolysis, which is compensated duly in tumor cells through overexpression of the glyoxalase enzyme system.³ Obstruction of the glyoxalase system in cancerous cells would lead to the induction of apoptosis in such cells because of the excessive intracellular accumulation of methylglyoxal. Our laboratory was the first to propose the inhibition of Glx-I as a means to induce apoptosis in cancerous cells and to pioneer the exploration of the *S*-alkyl derivatives of glutathione as competitive inhibitors of Glx-I, leading ultimately to a potent Glx-I inhibitor, *S*-*p*-bromobenzyl glutathione (**1**, PBBG,^a Figure 2).^{4,5} Unfortunately, **1** was recognized as a substrate by γ -glutamyltranspeptidase (γ -GT), resulting in a rapid cleavage of its

γ -glu-cys bond and thus the rapid loss of Glx-I inhibitory activity. A solution to this problem was found in the replacement of this labile linkage by a robust urea isostere, leading to a metabolically stable analogue (**2**, Figure 2), which retains the Glx-I inhibitory potency of the parent compound.⁶ On a separate note, Murthy and Creighton exploited successfully the Zn²⁺-chelating ability of the hydroxamate function in their design of enediol(ate) transition state analogue inhibitors of Glx-I, such as the *S*-(*N*-Aryl-*N*-hydroxycarbamoyl) derivatives of glutathione (e.g., **3**, Figure 2).⁷ The structural similarity borne by compounds such as **3** to glutathione made them function as substrates of γ -GT, making them extremely labile. Furthermore, Creighton et al. have shown that the similarity of the thiohydroxamates to *S*-lactoyl glutathione make compounds like **3** function as substrates of Glx-II.^{8,9} We reported recently the union of these two distinct strategies represented by **4** (Figure 2), the urea-isostere analogue of **3**, that is resistant to γ -GT-mediated breakdown.¹⁰ We next decided to focus our efforts on simplifying the structural scaffolding of these hydroxamate inhibitors from a synthetic viewpoint. The growing synthetic complexity of these systems due to the thiohydroxamate linkage, in addition to its potential instability, also made the replacement of this link particularly attractive.

The present study was aimed, at least at the outset, to identify isosteric replacements for the thiohydroxamate linkage that would improve the facility of the synthesis of the resultant analogues while retaining their potency against Glx-I and stability toward γ -GT.

Structural Iteration I. Replacement of Sulfur by Methylene. Rationale. We turned our attention first to the replacement of the thiocarbamate linkage in inhibitors like **3** and **4**. The X-ray crystal structure of a hydroxamate ligand bound to Glx-I, as described by Cameron and Mannervik, was not suggestive of any specific conformational, electronic, or spatial elements of recognition contributed by the sulfur atom.¹¹ Replacement of this sulfur atom by a carbon would remove the thioester structural motif, potentially rendering the resultant carbo-analogue resistant to Glx-II. Ly et al. have demonstrated the utility of such an approach in the

*To whom correspondence should be addressed. Phone: 612-624-9911. Fax: 612-624-0139. E-mail: vince001@umn.edu.

^a Abbreviations: Glx-I, glyoxalase I; Glx-II, glyoxalase II; γ -GT, γ -glutamyltranspeptidase; PBBG, *S*-*p*-bromobenzyl glutathione.

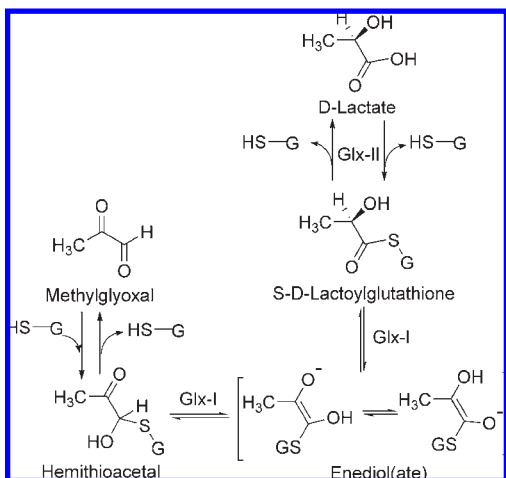


Figure 1. The glyoxalase system.

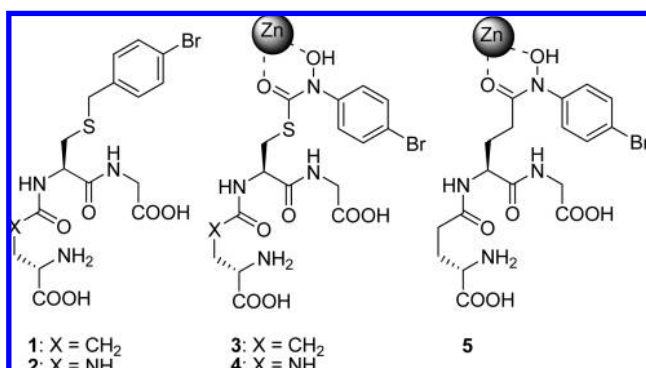


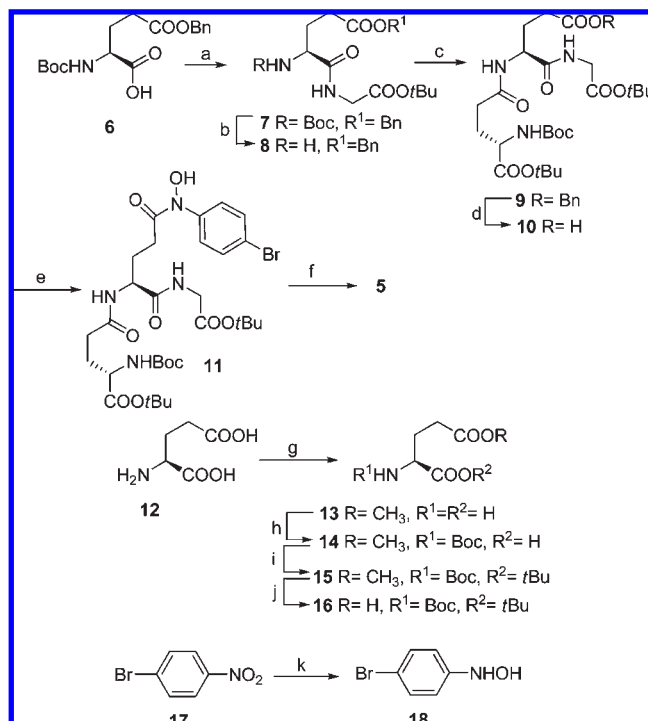
Figure 2. Developments in the design of glyoxalase I inhibitors.

inhibition of Glx-I.¹² In addition, the appropriate residue that bears the hydroxamate appendage in the carbo-analogues would be glutamic acid, creating a point of synthetic entry. We therefore set forth to synthesize **5** (the carbo-analogue of **3**), which embodies this change.

Synthesis of 5. Compound **5** was approached through the synthesis of a suitably protected tripeptide backbone (Glu-Glu-Gly), followed by coupling of the γ -carboxylic acid of the central glutamic acid to an aryl-hydroxylamine. As shown in Scheme 1, synthesis of compound **5** began with the coupling of commercially available *N*-Boc-5-benzyl ester of glutamic acid (**6**) with glycine *tert*-butyl ester to give dipeptide **7**. Selective Boc-deprotection over the *tert*-butyl ester¹³ (Hruby's conditions) and the coupling of the resulting dipeptide amine **8** with *N*-Boc-1-*tert*-butyl ester of glutamic acid (**16**) afforded the tripeptide **9**. Compound **16** in turn was prepared from *L*-glutamic acid through a four-step sequence. Finally, hydrogenolysis of the side chain benzyl ester of the tripeptide **9** provided acid **10**.

p-Bromophenylhydroxylamine (**18**, an unstable solid) was synthesized by a Rh-catalyzed transfer hydrogenation ("diimide reduction") of 4-bromonitrobenzene (**17**).¹⁴ Results of attempted coupling of **18** with acid **10** under varying reaction temperatures were suggestive of appreciable degradation of hydroxylamine **18** at room temperature, especially in the presence of tertiary amines. The precise chemical nature of the degradation, however, was intractable. Hence our next attempts utilized low reaction temperatures with the absence of any tertiary amine base. DCC coupling at 0–4 °C for 6 h, which does not require any tertiary amine base, was

Scheme 1. Synthesis of Hydroxamate-Based Glyoxalase I Inhibitor **5**^a



^a Reagents and conditions: (a) HCl·H₂N-Gly-OtBu, EDC, HOBT, NMM, CH₂Cl₂, 91%; (b) 4 N HCl/dioxane, 0 °C, 99%; (c) **16**, EDC, HOBT, NMM, CH₂Cl₂, 84%; (d) H₂, 10% Pd/C, CH₃OH, 86%; (e) **18**, EDC, CH₂Cl₂, 52%; (f) TFA, CH₂Cl₂ (1:1), 76%; (g) TMSCl, CH₃OH, 97%; (h) Boc₂O, NaHCO₃, dioxane/H₂O (2:1), 91%; (i) *t*BuOH, DCC, DMAP, 94%; (j) LiOH, THF/H₂O (3:1), 84%; (k) 5% Rh-C, NH₂NH₂·H₂O, THF, 71%.

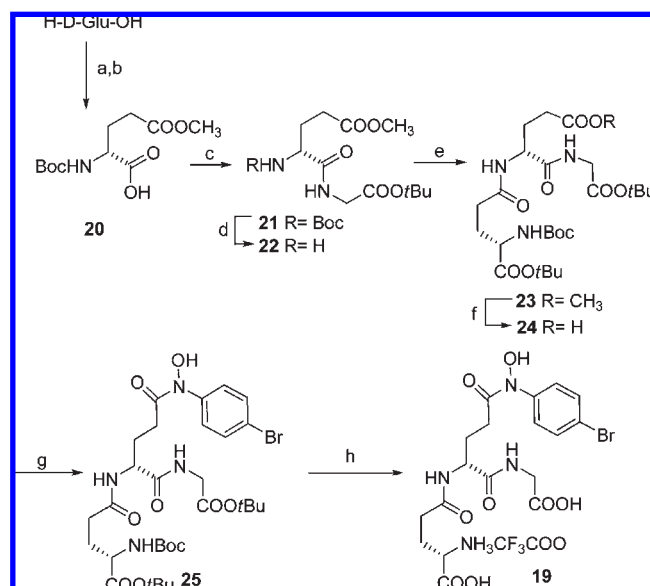
attempted but it gave the coupled product **11** as an inseparable mixture with DCU. Finally, this problem was overcome by utilizing a combination of EDC and a 5-fold excess of amine **18** at 0–4 °C to give the pure product **11** in 61% yield. Global deprotection of hydroxamate **11** with trifluoroacetic acid gave the target **5** as its CF₃COOH salt.

Evaluation of 5 and Resulting Implications. Compound **5** was evaluated for its ability to inhibit yeast glyoxalase I, along with compounds **1–4** for comparison. The isomerization process leading to the formation of *S*-D-lactoyl glutathione is accompanied by an increase in the absorption at 240 nm. This increase in UV absorption for the first 6 min was utilized as a gauge to calculate initial rate of the enzymatic reaction. Concentrations of the hemimercaptal formed by equilibration of methylglyoxal and GSH in the presence and absence of an inhibitor were calculated using the previously determined dissociation constant of 3.1×10^{-3} M.⁵ As seen in Table 1, **5** carries a spectacular increase in potency over **3** and **4**. With an inhibition constant of 6.17 ± 1.64 nM, it effectively is the most potent inhibitor of Glx-I known to date and is 1000-fold more potent than the parent thiocarboxamate analogue **3**. Kinetic experiments indicate that **5** is a tight-binding inhibitor of Glx-I.

The stability of **5** toward γ -glutamyltranspeptidase mediated cleavage was then determined next by its incubation at 37 °C with equine kidney γ -glutamyltranspeptidase (γ -GT, Sigma) at pH = 8.4 (Supporting Information, Figure S1).⁶ Inhibitor **5** underwent facile breakdown at its γ -Glu-Glu bond with incubated with γ -GT, indicating that this

Table 1. Inhibitory Constants (K_i) of Glyoxalase I Inhibitors 1–5

inhibitor	$K_i \pm \text{SEM} (\mu\text{M})$	
	(experimental)	(from literature)
1	6.28 ± 1.45	9.14 ± 1.30^6
2	12.8 ± 3.23	15.5 ± 3.10^6
3	1.15 ± 0.46	1.20 ± 0.20^7
4	2.19 ± 0.57^{11}	2.19 ± 0.57^{11}
5	0.00617 ± 0.00164	

Scheme 2. Synthesis of the Glyoxalase I Inhibitor **19**^a

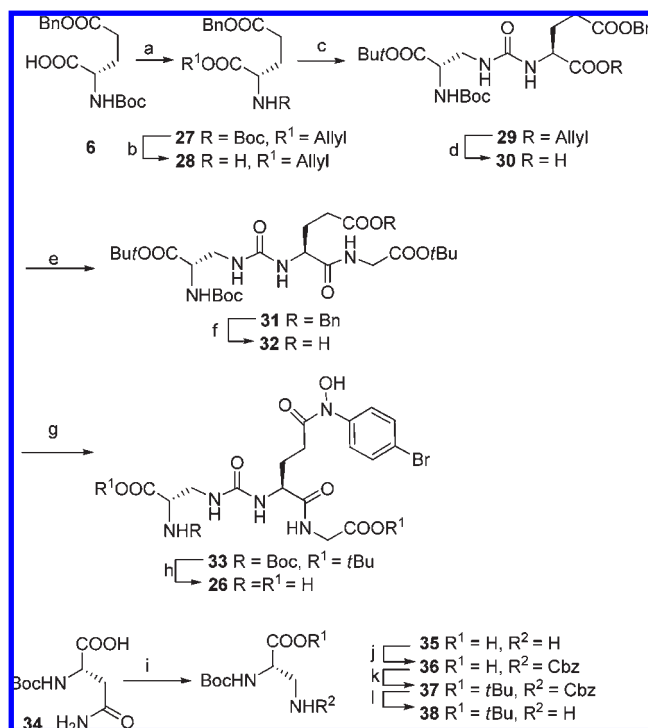
^a Reagents and conditions: (a) TMSCl, CH₃OH, 98%; (b) Boc₂O, NaHCO₃, dioxane-H₂O (2:1), 86%; (c) HCl·H₂N-Gly-OtBu, EDC, HOBT, NMM, CH₂Cl₂, 88%; (d) 4 N HCl/dioxane, 0 °C, 95%; (e) **16**, EDC, HOBT, NMM, CH₂Cl₂, 34%; (f) LiOH, THF/H₂O (1:1), 91%; (g) **18**, EDC, CH₂Cl₂, 62%; (h) TFA, CH₂Cl₂ (1:1), 79%.

breakdown should necessarily be the subject of the next structural iteration (Supporting Information, Figure S1).

Structural Iteration II. Building Resistance toward γ -GT. It is known that most proteases do not recognize unnatural enantiomers of amino acids at the cleavage sites. We designed compound **19** (Scheme 2), which bears a D-glu residue at the site of cleavage. This compound was approached through a synthetic route similar to that for **5** (Scheme 2). The δ -methyl ester of Boc-D-glutamic acid was utilized as the starting material.

Upon evaluation for Glx-I-inhibitory properties, the potency of **19** was found to be $1.66 \pm 0.67 \mu\text{M}$, about 1000-fold lower than its L-counterpart, **5**. Inhibitor **19** was indeed found to be resistant toward breakdown by γ -GT (Supporting Information, Figure S1). It is thus evident that the stereochemical requirements at the central residue for recognition at the active site of Glx-I are stringent; in other words, the potency of **5** most likely is a result, in part, of a well-defined conformation.

Toward the end of imparting γ -GT resistance to **5**, we also employed our previously described strategy of substituting the labile link by a ureide isostere, leading to compound **26**. The synthesis of **26**, as shown in Scheme 3, begins from **6** and proceeds via the dipeptide **29**, the ureide formed by the union of **28** and the diaminopropanoic acid derivative **38**.¹⁵ The compound **38** was in turn formed through the PIDA-mediated Hoffman degradation of the asparagine **34**

Scheme 3. Synthesis of the Glyoxalase I Inhibitor **26**^a

^a Reagents and conditions: (a) allyl bromide, benzene, reflux, 92%; (b) 4 N HCl/dioxane, 96%; (c) **38**, CDI, NMM, CH₂Cl₂, 82%; (d) (PPh₃)₄Pd, morpholine, CH₂Cl₂; (e) HCl·H₂N-Gly-OtBu, EDC, HOBT, NMM, CH₂Cl₂, 76% over two steps; (f) H₂, 10% Pd/C, CH₃OH, 89%; (g) **18**, EDC, CH₂Cl₂, 64%; (h) TFA, CH₂Cl₂ (1:1), 78%; (i) PIDA, EtOAc/CH₃CN/H₂O (2:2:1), 67%; (j) CbzCl, KOH, K₂CO₃, THF/H₂O (3:1), 94%; (k) *t*BuOH, DCC, DMAP, CH₂Cl₂, 84%; (l) H₂, 10% Pd/C, CH₃OH, 94%.

followed by suitable functionalization as described in our previous report.¹⁶ The allyl ester function of **29** was cleaved in the presence of the benzyl ester with (Ph₃P)₄Pd, and the resultant carboxylic acid was coupled to H-Gly-OtBu giving **31**. Hydrogenolysis of **31** and subsequent coupling to **18** afforded **33**, which was subjected to global deprotection with TFA to afford **26**·CF₃COOH. Compound **26** was found to retain the strong inhibitory properties of **5**; it inhibits Glx-I with a K_i of $32.6 \pm 4.17 \text{ nM}$. In addition, **26** was found to be expectedly stable toward γ -GT mediated breakdown (Supporting Information, Figure S1).

Structural Iteration III. Stabilizing the Hydroxamate Linkage. Having addressed successfully the problem of γ -GT mediated breakdown, we next turned our attention to the instability of the hydroxamate itself. We and others have observed that this linkage itself is susceptible to uncatalyzed hydrolytic breakdown, caused in part due to the fact that the anilino nitrogen of the hydroxamate is a good leaving group.^{17,18} This problem has previously been addressed by Michaelides et al. through reversal of the elements in relation with the scaffold, leading to “retro hydroxamates”, which were found to have superior stability toward hydrolytic breakdown.¹⁹ We decided to examine the effect of such a substitution on **5**, thusly leading to compound **39** (Figure 3).

Synthesis of 39. Our first attempts at the synthesis of the retrohydroxamate bearing residue were focused on the alkylation of *N-p*-bromobenzoyl-*O*-benzyl hydroxylamine with derivatives of homoserine (Scheme 4).²⁰ The allyl ester of

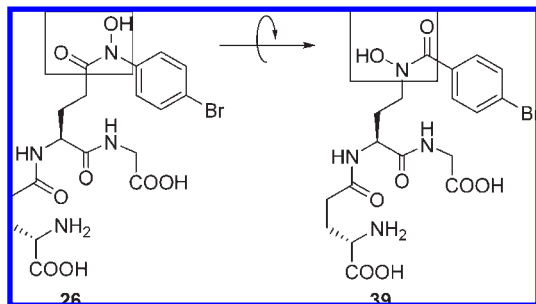
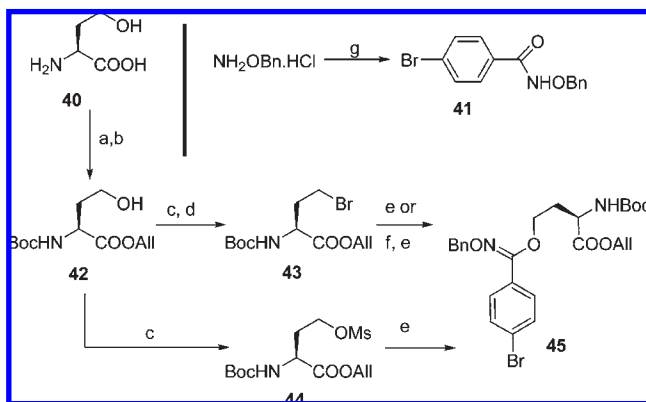


Figure 3. Design of retrohydroxamate **39** based on Michaelides' concept.

Scheme 4. Alkylation of **41** with Homoserine Electrophiles^a



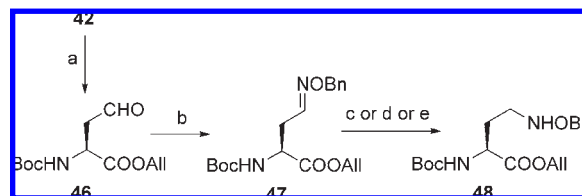
^a Reagents and conditions: (a) Boc_2O , NaOH , $\text{H}_2\text{O}/\text{CH}_3\text{CN}$ (1:1); (b) allyl bromide, DMF , 60% over two steps; (c) MsCl , Et_3N , CH_2Cl_2 ; (d) LiBr , acetone, 94% over two steps; (e) **41**, NaH , DMF ; (f) NaI , acetone, reflux, 89%.

Boc-homoserine, **42**, was elaborated into the corresponding bromide **43** and mesylate **44** derivatives. Treatment of the sodium imidate of **41** with these electrophiles led to **45**, whose $\delta\text{-CH}_2$ ^1H resonances appeared at 4.20–4.50 ppm (COSY assignment) with a corresponding ^{13}C resonance at 153.0 ppm (HMBC assignment). These values are not in agreement with the expected *N*-alkylated product, but rather, it seemed that predominant *O*-alkylation had occurred. We also attempted to introduce the retrohydroxamate through reductive amination of glutamic acid semialdehyde **46**.²¹ Although we could form the oxime **47**, we found impossible the reduction of **47** to **48**; NaBH_4 and NaCNBH_3 led to intractable mixtures while $\text{Na}(\text{OAc})\text{BH}_3$ failed to react with **47** (Scheme 5).

Reasoning that the formation of imidate **45** was enhanced by the electron-withdrawing nature of the bromobenzoyl substituent, we attempted to indirectly incorporate the retrohydroxamate through the corresponding Cbz-derivative. As shown in Scheme 6, such an alkylation indeed occurred on the nitrogen. However, the deprotected residue **51** underwent predominantly a Cbz-migration to **53** when its acylation was attempted, with no trace of the required dipeptide **52** detected.

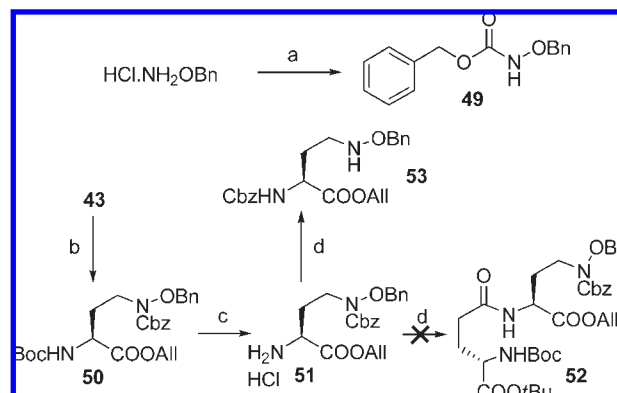
To bypass this migration, we synthesized the dipetide **54** instead, which underwent substitution with **49** to afford **55** (Scheme 7). Elaboration of **55** to the tripeptide **57** was also found to proceed uneventfully. Unfortunately, we could not cleave selectively the Cbz-protective group of **57**, with **58** being the predominant product. This persisted even when an inhibitor (CHCl_3) was added to the reaction. In the latter

Scheme 5. Attempted Reductive Amination of **46**^a



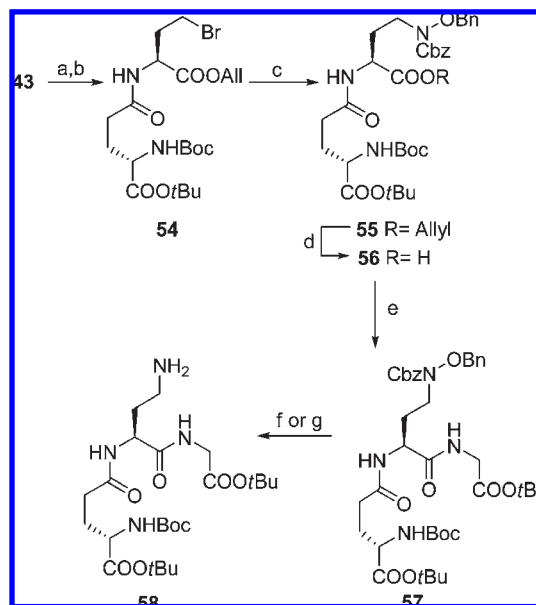
^a Reagents and conditions: (a) DMP , CH_2Cl_2 , 82%; (b) $\text{HCl}\cdot\text{H}_2\text{-NOBn}$, Et_3N , CH_2Cl_2 ; (c) NaCNBH_3 , CH_3COOH ; (d) NaBH_4 , CH_3OH ; (e) $\text{NaBH}(\text{OAc})_3$.

Scheme 6. Synthesis of **51** and Its Conversion to **53**^a



^a Reagents and conditions: (a) CbzCl , DIPEA , CH_2Cl_2 , 85%; (b) NaH , DMF , **53**, 89%; (c) 4 N HCl /dioxane, 95%; (d) **18**, EDC , HOBT , NMM , CH_2Cl_2 .

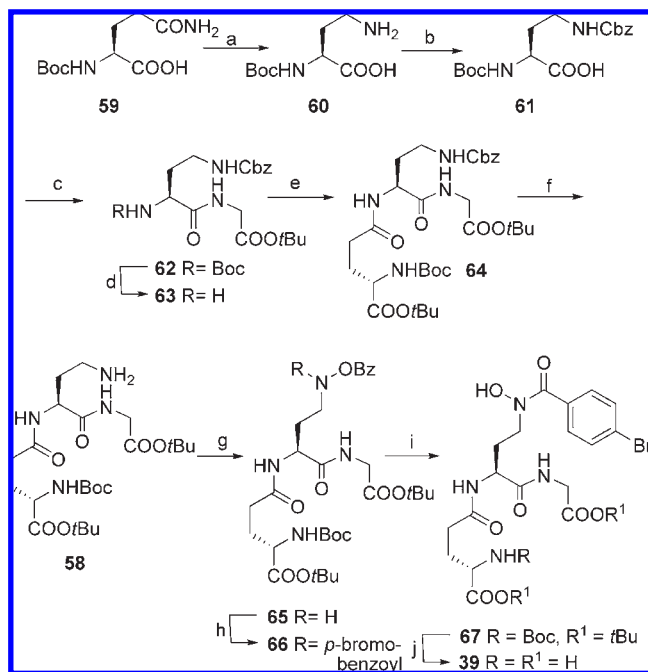
Scheme 7. Synthesis and Unsuccessful Selective Hydrogenation of **57**^a



^a Reagents and conditions: (a) 4 N HCl /dioxane, 95%; (b) **16**, PyAOP , Et_3N , CH_2Cl_2 , 82%; (c) NaH , DMF , **49**, 76%; (d) $\text{Pd}(\text{PPh}_3)_4$, morpholine, CH_2Cl_2 , 94%; (e) $\text{HCl}\cdot\text{H}_2\text{-N-Gly-OtBu}$, EDC , HOBT , NMM , CH_2Cl_2 , 72%; (f) H_2 , 10% Pd/C , CH_3OH , 88%; (g) H_2 , 10% Pd/C , 10% CHCl_3 in CH_3OH .

case, the reaction was indeed retarded but the product composition was unchanged.

The amine tripeptide **58** obtained in Scheme 6 was exploited for possible oxidation to the desired hydroxylamine **65**.

Scheme 8. Direct Oxidation of Primary Amine: A Successful Approach for the Synthesis of Retrohydroxamate Inhibitor **39**^a

^a Reagents and conditions: (a) PIDA, THF/H₂O (2:1), 76%; (b) CbzCl, K₂CO₃, THF/H₂O (3:1), 81%; (c) HCl·H₂N-Gly-OtBu, EDC, HOBt, NMM, CH₂Cl₂, 88%; (d) 4 N HCl/dioxane, 0 °C; (e) **16**, EDC, HOBt, NMM, CH₂Cl₂, 76% over two steps; (f) H₂, 10% Pd/C, CH₃OH, 96%; (g) benzoylperoxide, carbonate buffer/CH₂Cl₂ (1:1); (h) 4-bromobenzoyl chloride, carbonate buffer/CH₂Cl₂, 71% over two steps; (i) 10% NH₄OH/CH₃OH, 82%; (j) TFA, CH₂Cl₂ (1:1), 70%.

In 1978, Naegeli and Keller-Schierlein²² reported an elegant total synthesis of D-ferrichrome by an indirect oxidation of primary amine to hydroxylamine.²³ Their indirect oxidation featured the conversion of primary amines to imines followed by oxidation of imines to oxaziridines. Aminolysis of oxaziridines afforded hydroxylamines, which led to the successful synthesis of D-ferrichrome. This indirect oxidation though an attractive approach for obtaining our reverse-amide hydroxamate scaffold was unsuccessful in our hands. However, another promising alternative was to use direct oxidation protocol of Nemchik and Phanstiel^{24,25} that utilizes benzoyl peroxide as an oxidant.

The tripeptide amine **58** required for this transformation was obtained in large scale starting with L-glutamine (**59**, Scheme 8). Hoffman rearrangement of primary amide in glutamine²⁶ resulted in amine **60**, which was subjected to Cbz-protection. The acid **61** thus obtained was coupled to glycine *tert*-butyl ester, resulting in dipeptide **62**. *N*-Boc-deprotection followed by coupling of dipeptide **62** with Boc-Glu-*tert*-butyl ester **27** offered the tripeptide **64**. Hydrogenolysis of Cbz-group gave the primary amine **58**, which was subjected to BPO-mediated oxidation.^{27,28} Indeed, this protocol gave the desired *O*-benzoylhydroxylamine tripeptide **65** along with ~5% yield of benzoylated derivative of the primary amine **58** due to its acylation with BPO. The tripeptide hydroxylamine **65** was subjected without isolation to acylation with *p*-bromobenzoyl bromide, resulting in tripeptide **66**. Benzoyl ester functionality in **66** was hydrolyzed with ammonium hydroxide, resulting in hydroxamate **67**.²⁷ Finally, concomitant deprotection of *N*-Boc and *tert*-butyl functional groups gave the target compound **39** as its trifluoroacetate salt.

Compound **39** was found to indeed inhibit Glx-I and was a tight-binding inhibitor with potency in the nanomolar range ($K_i = 123 \pm 5.36$ nM). Compound **39** was, in addition, found to resist uncatalyzed hydrolytic cleavage, validating the rationale for its design (Supporting Information, Figure S1).

Discussion

This study has lent, perhaps through sheer serendipity, the first low-nanomolar inhibitor of glyoxalase I (inhibitor **5**). We have also been able to examine the effect of various modifications of **5** on potency as well as stability. Our previously reported ureide-isostere strategy was found to be applicable to **5**, conferring on this novel class of inhibitors the much needed stability toward γ -GT mediated breakdown. Reversal of the atom-order in the hydroxamate function led to the identification of the lead inhibitor **39**, that possesses stability toward hydrolytic breakdown. Of much interest is the loss of potency observed when the configuration about the α -carbon of the central residue was inverted because this is indicative of a well-defined conformation being necessary for recognition of inhibitors such as **5** at the active site of Glx-I. It may be worthwhile at this juncture to the design and synthesize constrained molecules in order to delineate the optimal conformation.

The peptidic nature of inhibitors as well as low potency has precluded further research in the area of glyoxalase I inhibition for a number of years. It is expected that the information garnered from the studies in this report would be useful toward the design and synthesis of inhibitors with higher conformational definition and lower peptidic character, which translate to higher potency and more favorable pharmacokinetics.

Experimental Section

TFA·H₂N- γ -Glu[*-*Glu(CON(OH)-*p*-bromophenyl)-Gly-OH]-OH (5**).** The protected tripeptide **19** (100 mg, 0.14 mmol) was added to a mixture of TFA and CH₂Cl₂ (1:1 v/v, 6 mL) and stirred at room temperature for 4 h. Concentration of the reaction mixture and trituration of the residue with ether and EtOAc afforded a light-brown solid. Recrystallization of this solid by dissolution into 50% ethanol and cooling in ice gave analytically pure **5** (65 mg, 76% yield). R_f 0.50 (butanol/acetic acid/H₂O, 12:5:3); $[\alpha]_D -15.4$ (*c* 0.5, 1N HCl). ¹H NMR (300 MHz, CD₃OD/CF₃COOD) δ 7.58–7.32 (bd, 4H, Ar), 4.41 (m, 1H, α -CH:Glu), 3.96–3.74 (m, 3H, α -CH:Glu, CH₂:Gly), 2.81–2.62 (m, 2H, γ -CH₂:Glu), 2.54–2.39 (m, 2H, γ -CH₂:Glu), 2.20–1.94 (m, 4H, β -CH₂:Glu). ¹³C NMR (75 MHz, CD₃OD/CF₃COOD) δ 173.9, 173.8, 172.9, 171.8, 167.4 (C(=O)), 138.4, 131.8, 123.6, 119.2 (C_{Ar}), 54.2, 53.6 (α -C:Glu), 42.3 (CH₂:Gly), 32.8, 30.6, 28.7, 27.5 (β -C:Glu, γ -C:Glu). ESI-HRMS m/z 503.0767 (M+H)⁺; C₁₈H₂₃BrN₄O₈ + H⁺ requires 503.0778. Reverse phase HPLC was run on Varian Microsorb column (C18, 5 μ m, 4.6 mm \times 250 mm) using two solvent systems with 0.5 mL/min flow rate and detected at 254 nm. Solvent system 1: 0.04 M TEAB (triethylammonium bicarbonate) in water/70% acetonitrile in water = 1/1, t_R = 6.96 min, purity = 98.6%. Solvent system 2: 0.04 M TEAB in water/70% acetonitrile in water = 20–100% B linear, t_R = 13.12 min, purity = 99.5%.

TFA·NH₂- γ -Glu[*-*D-Glu(CON(OH)-*p*-bromophenyl)-Gly-OH]-OH (19**).** The protected tripeptide **20** (100 mg, 0.14 mmol) was added to a 50% solution of TFA in CH₂Cl₂. After 4 h at room temperature, the reaction mixture was evaporated to dryness and triturated with EtOAc and ether to get a white solid. Recrystallization of this solid from 50% ethanol gave analytically pure **6** (68 mg, 79% yield). R_f 0.50 (butanol/acetic acid/H₂O, 12:5:3); $[\alpha]_D +26.4$ (*c* 0.25, 1N HCl). ¹H NMR (300 MHz, CD₃OD/CF₃COOD)

δ 7.58–7.32 (bd, 4H, Ar), 4.41 (m, 1H, α -CH:Glu), 3.96–3.74 (m, 3H, α -CH:Glu, CH₂:Gly), 2.81–2.62 (m, 2H, γ -CH₂:Glu), 2.54–2.39 (m, 2H, γ -CH₂:Glu), 2.20–1.94 (m, 4H, β -CH₂:Glu). ¹³C NMR (75 MHz, CD₃OD/CF₃COOD) δ 173.9, 173.8, 172.9, 171.8, 167.4 (C=O), 138.4, 131.8, 123.6, 119.2 (C_{Ar}), 54.2, 53.6 (α -C:Glu), 42.3 (CH₂:Gly), 32.8, 30.6, 28.7, 27.5 (β -C:Glu, γ -C:Glu). ESI HRMS m/z 503.0754 (M + H)⁺; C₁₈H₂₃BrN₄O₈ + H⁺ requires 503.0778. HPLC purity (detected at 254 nm) = 99.4%. Reverse phase HPLC was run on Varian Microsorb column (C18, 5 μ m, 4.6 mm \times 250 mm) using two solvent systems with 0.5 mL/min flow rate and detected at 254 nm. Solvent system 1: 0.04 M TEAB (triethylammonium bicarbonate) in water/70% acetonitrile in water = 1/1, t_R = 5.31 min, purity = 99.4%. Solvent system 2: 0.04 M TEAB in water/70% acetonitrile in water = 20–100% B linear, t_R = 13.42 min, purity = 98.99%.

TFA·NH₂- γ -Glu[β -Glu(CON(OH)-*p*-bromophenyl)Gly-OH]-OH (26). A mixture of **36** (100 mg, 0.14 mmol) and TFA-CH₂Cl₂ (1:1 v/v, 6 mL) was stirred at room temperature for 4 h. After concentration, the residue was triturated with ether and EtOAc to get a white residue. Recrystallization by first dissolving in 0.1 N HCl at rt and then cooling in ice/salt gave analytically pure **7** (66 mg, 78% yield) as a feathery solid. R_f 0.55 (butanol/acetic acid/H₂O, 12:5:3); [α]_D –19.2 (*c* 0.5, 1 N HCl). ¹H NMR (300 MHz, CD₃OD/CF₃COOD) δ 7.59 (d, *J* = 9.0, 2H, Ar), 7.49 (d, *J* = 8.7 Hz, 2H, Ar), 4.60 (q, *J* = 4.8, 8.4 Hz, 1H, α -CH:Glu), 4.48 (q, *J* = 4.8, 7.8 Hz, 1H, α -CH:Dap), 4.17 (m, 2H, CH₂:Gly), 3.68–3.62, 3.41–3.34 (2m, 2H, β -CH₂:Dap), 3.24–2.98 (m, 2H, β -CH₂:Glu). ¹³C NMR (75 MHz, CD₃OD/CF₃COOD) δ 174.5, 172.6, 170.5, 159.2, 157.1 (C=O), 140.6 (C_{Ar}:NOH), 131.5 (C_{Ar}: ortho to Br), 121.1 (C_{Ar}:Br), 117.7 (C_{Ar}: ortho to NOH), 52.4 (α -C:Glu), 49.1 (α -C:Dap), 44.3 (β -C:Dap), 42.6 (CH₂:Gly), 31.5 (β -C:Glu). ESI-HRMS m/z 504.0740 (M + H)⁺; C₁₇H₂₂BrN₅O₈ + H⁺ requires 504.0730. Reverse phase HPLC was run on Varian Microsorb column (C18, 5 μ m, 4.6 mm \times 250 mm) using two solvent systems with 0.5 mL/min flow rate and detected at 254 nm. Solvent system 1: 0.04 M TEAB (triethylammonium bicarbonate) in water/70% acetonitrile in water = 1/1, t_R = 7.00 min, purity = 96.06%. Solvent system 2: 0.04 M TEAB in water/70% acetonitrile in water = 20–100% B linear, t_R = 14.67 min, purity = 95.90%.

TFA·NH₂- γ -Glu[β -Dab(*N*-(*p*-bromobenzoyl)-*N*-hydroxyl)-Gly-OH]-OH (39). Protected tripeptide **68** (100 mg, 0.14 mmol) was treated with a mixture of TFA and CH₂Cl₂ (1:1 v/v, 6 mL) at room temperature for 4 h. The reaction mixture was then concentrated and the residue obtained was triturated with ether and EtOAc to afford a white solid. Recrystallization of the TFA salt from 0.1 N HCl aqueous gave analytically pure **8** (60 mg, 70% yield). R_f 0.60 (butanol/acetic acid/H₂O, 12:5:3); [α]_D –12.6 (*c* 0.44, 1 N HCl). ¹H NMR (300 MHz, CD₃OD/CF₃COOD) δ 7.59 (d, *J* = 9.0, 2H, Ar), 7.49 (d, *J* = 8.7 Hz, 2H, Ar), 4.43 (m, 1H, α -CH:Glu), 4.17–3.89 (m, 3H, α -CH:Dab, CH₂:Gly), 3.44 (m, 2H, γ -CH₂:Dab), 2.55–1.89 (m, 6H, β -CH₂:Dab, β -CH₂:Glu, γ -CH₂:Glu). ¹³C NMR (75 MHz, CD₃OD/CF₃COOD) δ 173.5, 173.1, 172.6, 170.3, 167.2 (C=O), 139.7, 130.8, 123.7, 119.4 (C_{Ar}), 54.1, 52.4 (α -C:Glu, α -C:Dab), 46.4 (γ -C:Dab), 42.4 (CH₂:Gly), 31.9 (γ -C:Glu), 28.7, 23.2 (β -C:Glu, β -C:Dab). ESI-HRMS m/z 503.0751 (M + H)⁺; C₁₈H₂₃BrN₄O₈ + H⁺ requires 503.0772. Reverse phase HPLC was run on Varian Microsorb column (C18, 5 μ m, 4.6 mm \times 250 mm) using two solvent systems with 0.5 mL/min flow rate and detected at 254 nm. Solvent system 1: 0.04 M TEAB (triethylammonium bicarbonate) in water/70% acetonitrile in water = 1/1, t_R = 5.45 min, purity = 96.65%. Solvent system 2: 0.04 M TEAB in water/70% acetonitrile in water = 20–100% B linear, t_R = 6.86 min, purity = 95.07%.

Glyoxalase I Enzyme Kinetics Assay. The glyoxalase I inhibitors were tested for their ability to inhibit yeast glyoxalase I in an enzyme kinetic assay. Yeast glyoxalase I and the substrate methylglyoxal were purchased from Sigma Chemical Co. The commercial 40% methylglyoxal solution was distilled to remove

polymerization product and then diluted with distilled water. The acidic impurities were removed by passing the diluted distillate through Amberlite-400 resin (carbonate form, prepared by stirring 450 mL of chloride form of resin with an aqueous solution containing 40 g of Na₂CO₃). The methyl glyoxal solution thus obtained after filtering off the resin was standardized by the method of Friedemann.²⁹ Enzyme assays were performed (30 °C, 0.05 M phosphate buffer (pH 6.6)) using a thermostatted Beckman DU 7400 spectrophotometer. A fresh GSH solution was prepared, on the day of the assays, using distilled, deionized water. For each assay, the cell contained a total volume of 3.0 mL, which was no more than 6.0 mM with respect to methylglyoxal and 1.3 mM with respect to GSH. Sufficient amounts of glyoxalase I, in the presence of 0.1% bovine serum albumin (Sigma) as a stabilizing agent, were employed to give an easily measurable initial rate, which was followed by an increase in absorption at 240 nm. Stock inhibitor solutions were prepared in the distilled water and adjusted, when necessary, to pH 6.6. Methylglyoxal, GSH, and buffer (and inhibitor) were added to a cuvette and allowed to stand for 6 min in the thermostatted compartment of the spectrophotometer to allow complete hemimercaptal equilibration. Hemimercaptal substrate concentrations were calculated from the concentrations of GSH and methylglyoxal added, using a value of 3.1×10^{-3} M for the dissociation constant of the hemimercaptal at pH 6.6. Data were analyzed using an Enzyme kinetics module of Sigmaplot 9.0 from Systat Software Inc.

γ -Glutamyltranspeptidase Assay. The stability of glyoxalase I inhibitors toward γ -GT mediated degradation was determined by incubating 100 μ L of 10 mM solutions of these inhibitors (dissolved in 200 mM of 2-amino-2-methyl-1,3-propanediol buffer at pH 8.5) with 10 μ L of 0.54 mg/100 μ L equine kidney γ -glutamyltranspeptidase in the above buffer in presence of 20 μ L of acceptor dipeptide gly gly (40 mM in the above buffer). At selected time intervals, a compound from each tube was spotted on silica gel TLC plate during its incubation at 37 °C. Thin layer chromatography of these samples was performed on silica gel TLC plates and compared with the authentic predicted degradation products (solvent system: (6:2.5:1.5) butanol/acetic acid/water). Visual detection of TLC spots was performed under UV and also by iodine and fluorescamine staining solution.

Acknowledgment. This work was supported financially by a grant from the Center for Drug Design, Academic Health Center, University of Minnesota. We thank Jay Brownell for his guidance while performing the glyoxalase I enzyme kinetics assays.

Supporting Information Available: Experimental details for the synthesis of all new compounds and thin-layer chromatograms for the γ -glutamyltranspeptidase assay. This material is available free of charge via the Internet at <http://pubs.acs.org>.

References

- (1) Ramasamy, R.; Vannucci, S. J.; Yan, S. S.; Herold, K.; Yan, S. F.; Schmidt, A. M. Advanced glycation end products and RAGE: a common thread in aging, diabetes, neurodegeneration, and inflammation. *Glycobiology* **2005**, *15*, 16R–28R.
- (2) Thornalley, P. J. The glyoxalase system: new developments towards functional characterization of a metabolic pathway fundamental to biological life. *Biochem. J.* **1990**, *269*, 1–11.
- (3) Antognelli, C.; Baldracchini, F.; Talesa, V. N.; Costantini, E.; Zucchi, A.; Mearini, E. Overexpression of glyoxalase system enzymes in human kidney tumor. *Cancer J.* **2006**, *12*, 222–228.
- (4) Vince, R.; Wadd, W. B. Glyoxalase Inhibitors as Potential Anticancer Agents. *Biochem. Biophys. Res. Commun.* **1969**, *35*, 593–598.
- (5) Vince, R.; Daluge, S.; Wadd, W. B. Inhibition of Glyoxalase I by S-Substituted Glutathiones. *J. Med. Chem.* **1971**, *14*, 402–404.
- (6) Vince, R.; Brownell, J.; Akella, L. B. Synthesis and Activity of γ -(L- γ -azaglutamyl)-S-(*p*-bromobenzyl)-L-cysteinylglycine: A Metabolically

- Stable Inhibitor of Glyoxalase I. *Bioorg. Med. Chem. Lett.* **1999**, *9*, 853–856.
- (7) Murthy, N. S. R. K.; Bakeris, T.; Kavarana, M. J.; Hamilton, D. S.; Lan, Y.; Creighton, D. J. *S*-(*N*-Aryl-*N*-hydroxycarbonyl)glutathione Derivatives Are Tight-Binding Inhibitors of Glyoxalase I and Slow Substrates for Glyoxalase II. *J. Med. Chem.* **1994**, *37*, 2161–2166.
- (8) Hamilton, D. S.; Creighton, D. J. Inhibition of Glyoxalase I by The Enediol Mimic *S*-(*N*-hydroxy-*N*-methylcarbonyl)glutathione. The Possible Basis of a Tumor-Selective Anticancer Strategy. *J. Biol. Chem.* **1992**, *267*, 24933–24936.
- (9) Zheng, Z. B.; Creighton, D. J. Bivalent Transition-State Analogue Inhibitors of Human Glyoxalase I. *Org. Lett.* **2003**, *5*, 4855–4858.
- (10) More, S. S.; Vince, R. A Metabolically Stable Tight-binding Transition-State Inhibitor of Glyoxalase-I. *Bioorg. Med. Chem. Lett.* **2006**, *16*, 6039–6042.
- (11) Cameron, A. D.; Ridderstrom, M.; Olin, B.; Kavarana, M. J.; Creighton, D. J.; Mannervik, B. Reaction Mechanism of Glyoxalase I Explored by an X-ray Crystallographic Analysis of the Human Enzyme in Complex with a Transition State Analogue. *Biochemistry* **1999**, *38*, 13480–13490.
- (12) Ly, H. D.; Clugston, S. L.; Sampson, P. B.; Honek, J. F. Syntheses and Kinetic Evaluation of Hydroxamate-Based Peptide Inhibitors of Glyoxalase I. *Bioorg. Med. Chem. Lett.* **1998**, *8*, 705–710.
- (13) Han, G.; Tamaki, M.; Hruby, V. J. Fast, Efficient and Selective Deprotection of the *tert*-Butoxycarbonyl (Boc) Group using HCl/dioxane (4 M). *J. Pept. Res.* **2001**, *58*, 338–341.
- (14) Oxley, P. W.; Adger, B. M.; Sasse, M. J.; Forth, M. A. *N*-Acetyl-*N*-phenylhydroxylamine via Catalytic Transfer Hydrogenation of Nitrobenzene Using Hydrazine and Rhodium on Carbon. *Org. Synth.* **1989**, *67*, 187–192.
- (15) Zhang, X.; Rodrigues, J.; Evans, L.; Hinkle, B.; Ballantyne, L.; Pena, M. Formation of Urea Dipeptides from Carbonyldiimidazole: Application toward the Protease Inhibitors GE 20372 and MAPI. *J. Org. Chem.* **1997**, *62*, 6420–6423.
- (16) More, S. S.; Vince, R. Design, Synthesis and Biological Evaluation of Glutathione Peptidomimetics as Components of Anti-Parkinson Prodrugs. *J. Med. Chem.* **2008**, *51*, 4581–4588.
- (17) Suzuki, T.; Miyata, N. Rational Design of Non-Hydroxamate Histone Deacetylase Inhibitors. *Mini-Rev. Med. Chem.* **2006**, *6*, 515–526.
- (18) Vassiliou, S.; Mucha, A.; Cuniassé, P.; Georgiadis, D.; Lucet-Levannier, K.; Beau, F.; Kannan, R.; Murphy, G.; Knaeuper, V.; Rio, M. C.; Basset, P.; Yiotakis, A.; Dive, V. Phosphinic Pseudo-Tripeptides as Potent Inhibitors of Matrix Metalloproteinases: A Structure–Activity Study. *J. Med. Chem.* **1999**, *42*, 2610–2620.
- (19) Michaelides, M. R.; Dellaria, J. F.; Gong, J.; Holms, J. H.; Bouska, J. J.; Stacey, J.; Wada, C.; Heyman, H. R.; Curtin, M. L.; Guo, Y.; Goodfellow, C. L.; Elmore, I. B.; Albert, D. H.; Magoc, T. J.; Marcotte, P. A.; Morgan, D. W.; Davidsen, S. K. Biaryl Ether Retrohydroxamates as Potent, Long-lived, Orally Bioavailable MMP Inhibitors. *Bioorg. Med. Chem. Lett.* **2001**, *11*, 1553–1556.
- (20) Carrasco, M. R.; Brown, R. T. A Versatile Set of Aminooxy Amino Acids for the Synthesis of Neoglycopeptides. *J. Org. Chem.* **2003**, *68*, 8853–8858.
- (21) Filira, F.; Biondi, B.; Giannini, E.; Gobbo, M.; Negri, L.; Rocchi, R. Opioid Peptides: Synthesis and Biological Properties of [(*N* γ -Glucosyl,*N* γ -methoxy)- α,γ -diamino-(*S*)-butanoyl]4-deltorphin-1-neoglycopeptide and Related Analogues. *Org. Biomol. Chem.* **2003**, *1*, 3059–3063.
- (22) Nægeli, H. U.; Keller-Schierlein, W. Stoffwechselprodukte Von Mikroorganismen. Eine Neue Synthese des Ferrichroms: Enantio-Ferrichrom. *Helv. Chim. Acta* **1978**, *61*, 2088–2095.
- (23) Lin, Y.; Miller, M. J. Practical Synthesis of Hydroxamate-Derived Siderophore Components by an Indirect Oxidation Method and Syntheses of a DIG–Siderophore Conjugate and a Biotin–Siderophore Conjugate. *J. Org. Chem.* **1999**, *64*, 7451–7458.
- (24) Nemchik, A.; Badescu, V.; Phanstiel, O. *N*-(Benzoyloxy)amines: An Investigation of Their Thermal Stability, Synthesis, and Incorporation into Novel Peptide Constructs. *Tetrahedron* **2003**, *59*, 4315–4325.
- (25) Wang, Q. X.; King, J.; Phanstiel, O. An Improved Synthesis of *O*-Benzoyl Protected Hydroxamates. *J. Org. Chem.* **1997**, *62*, 8104–8108.
- (26) Andruszkiewicz, R.; Rozkiewicz, D. An improved preparation of *N2-tert*-butoxycarbonyl- and *N2-benzyloxy-carbonyl*-(*S*)-2,4-diaminobutanoic acids. *Synth. Commun.* **2004**, *34*, 1049–1056.
- (27) Nemchik, A.; Badescu, V.; Phanstiel, O. *N*-(Benzoyloxy)amines: An Investigation of Their Thermal Stability, Synthesis, and Incorporation into Novel Peptide Constructs. *Tetrahedron* **2003**, *59*, 4315–4325.
- (28) Wang, Q. X.; King, J.; Phanstiel, O. An Improved Synthesis of *O*-Benzoyl Protected Hydroxamates. *J. Org. Chem.* **1997**, *62*, 8104–8108.
- (29) Friedemann, T. E. The Action of Alkali and Hydrogen Peroxide on Glyoxals. *J. Biol. Chem.* **1927**, *73*, 331–334.